

Evaluation of solid carvedilol-loaded SMEDDS produced by the spray drying method and a study of related substances

J. Mandić^{a,b}, I. Kosmač^{a,b}, M. Kovačević^a, B. Hodnik^b, Ž. Hodnik^b, F. Vrečer^{a,b}, M. Gašperlin^a,
B. Perissutti^c, A. Zvonar Pobirk^{a,*}

^a University of Ljubljana, Faculty of Pharmacy, Aškerčeva cesta 7, 1000 Ljubljana, Slovenia

^b Krka, d.d., Novo mesto, Šmarješka cesta 6, 8000 Novo mesto, Slovenia

^c University of Trieste, Dept. of Chemical and Pharmaceutical Sciences, P.le Europa 1, Trieste, Italy

ARTICLE INFO

Keywords:
SMEDDS
Carvedilol
Spray drying
Porous carriers
Stability
Related substances

ABSTRACT

In this study, various formulations of solidified carvedilol-loaded SMEDDS with high SMEDDS loading (up to 67% w/w) were produced with the spray drying process using various porous silica-based carriers. The process yield was improved with higher atomization gas flow rate during the spray drying process and with prolonged mixing time of dispersion of liquid SMEDDS and solid porous carriers prior to the spray drying process. Depending on the choice of the carrier and the SMEDDS:carrier ratio in solid SMEDDS, different drug loading, self-microemulsifying properties, drug release rates, and released drug fractions were obtained. The products exhibited fast drug release due to preserved self-microemulsifying properties and the absence of crystalline carvedilol, which was confirmed with XRD and Raman mapping. A decrease in drug content during the stability study was observed and investigated. This was at least partially attributed to the chemical degradation of the drug. Key degradation products determined by the LC-MS method were amides formed by in situ reaction of carvedilol with fatty acids present in the oily phase of SMEDDS.

1. Introduction

Self-microemulsifying drug delivery systems (SMEDDS) are complex lipid-based drug delivery systems composed of a mixture of oils (lipids), surfactants, and optionally co-surfactants and co-solvents that have great potential for enhancing the drug solubility and oral bioavailability of poorly water-soluble drugs, such as class II and class IV drugs of the biopharmaceutical classification system (BCS) (Čerpnjak et al., 2013). To enhance the stability of the incorporated drug and to avoid expensive capsule liquid-filling technology such as soft gel capsules, various solidification techniques are being explored, with the greatest interest in well-established industrially applicable technologies (Gonçalves et al., 2018; Mandić et al., 2017). One of them is spray drying (SD), a continuous, rapid, and scalable technology that has successfully been used for the production of solid SMEDDS (s-SMEDDS) in many studies (Li et al., 2013; Kim et al., 2015; Kang et al., 2012; Baek et al., 2015; Oh et al., 2011; Čerpnjak et al., 2015a). Self-emulsifying properties of s-SMEDDS produced with SD can be affected by variation of the process parameters. Čerpnjak et al. (2015b) have shown that the atomization

pressure and the SD feed flow rate (spray rate) had a significant influence on the mean droplet size and polydispersity index (PDI) after reconstitution of s-SMEDDS. A possible disadvantage of solidification by the SD method could be lower yield due to the loss of non-encapsulated free drug with the exhausted gas (Li et al., 2013; Singh et al., 2013a). It was shown that the choice of the carrier can affect drug release and its oral bioavailability (Kang et al., 2012; Baek et al., 2015), along with the droplet size of the (micro)emulsion formed after reconstitution by decreasing the concentration of surfactants or solvents in SMEDDS (Li et al., 2013). A disadvantage of using conventional excipients (such as lactose, maltodextrin, HPMC, MCC, etc.) as carriers is their low capacity for SMEDDS loading, which presents limitations for delivering a suitable amount of drug in a single dosage form. Porous carriers, such as silicon dioxide, magnesium aluminometasilicate, and calcium silicate, which are generally recognized as safe, exhibit great potential due to their large liquid adsorption capacity. They have been extensively investigated and effectively used as carriers to produce solid SMEDDS with the adsorption method (ADS) (Inugala et al., 2015; Krupa et al., 2015; Milović et al., 2012; Shazly and Mohsin, 2015; Weerapol et al., 2015). Their good

* Corresponding author.

E-mail address: alenka.zvonar-pobirk@ffa.uni-lj.si (A. Zvonar Pobirk).

compactibility and reported fast drug release rate, linked with high specific surface area and mesoporosity of the carriers (e.g., Neusilin® US2) (Gumaste et al., 2013; Mura et al., 2012), also makes them appealing for production of s-SMEDDS with SD technology (Bhandari et al., 2017). However, a possible disadvantage of porous silica-based carriers can be incomplete drug release (Agarwal et al., 2009; Chavan et al., 2015; Snela et al., 2019; Van Speybroeck et al., 2012; Yeom et al., 2016). Bolko Seljak et al. (2018) have done research comparing the drug release rate of SMEDDS adsorbed on magnesium aluminometasilicate (Neusilin® US2) versus amorphous silica (Syloid® 244FP). Inferior drug release from a Syloid® 244FP-based product was attributed to incomplete desorption of hydrophilic surfactants due to high affinity to the carrier. Moreover, the carrier's specific surface area and also the length and shape of pores could have a significant impact on dissolution behavior and drug release from solid SMEDDS produced with ADS (Agarwal et al., 2009; Weerapol et al., 2015; Gumaste and Serajuddin, 2017). Gumaste et al. (2017) highlighted the possibility that the extent of drug release can decrease progressively with storage time due to the migration of SMEDDS to formulation-free regions deeper inside the pores of the carrier (Neusilin® US2), depending on the relative hydrophilicity of the formulations. They proposed the idea of blocking the deepest pores with a suitable excipient to prevent SMEDDS from penetrating into those narrow pores and consequently obtain a higher extent of formulation desorption. By pre-coating Neusilin® US2 with PVP, complete drug release (>80%) was obtained even after 6 months of storage, which Gumaste et al. attributed to improved rehydration and allowing emulsification of the formulations within the larger pores.

In our study, the SD method was investigated for solidification of carvedilol-loaded SMEDDS, composed of 10% Capmul® MCM EP, 10% castor oil, 40% Kolliphor® RH 40, and 40% PEG 400, which was developed and characterized in our previous study (Mandić et al., 2019) and successfully solidified by pellet coating and fluid bed granulation (Mandić et al., 2020). Carvedilol (CARV) was chosen as a model drug due to its poor solubility, belonging to BCS class II, and long-term stability in tablet formulations (Brook et al., 2007). The aim of the study was production of s-SMEDDS with high SMEDDS loading via the SD method, along with obtaining a high process yield ($\geq 75\%$). Various porous silica-based carriers were used for solidification in different SMEDDS:carrier ratios (1:1, 1.5:1, and 2:1) due to their high liquid load capacity (Aeroperl® 300 Pharma, Florite® R, Neusilin® US2, Syloid® 244FP, and Syloid® XDP 3050). The influence of mixing time of SD dispersion on the process yield was studied. Moreover, the impact of formulation variables (carrier type and SMEDDS:carrier ratio) on the process yield, drug loading, self-microemulsifying properties, and drug-release profile and final drug quantity released from s-SMEDDS was investigated and compared. Carriers' pore prefilling with HPMC and drug-free SMEDDS was investigated as means of enhancing relative CARV content in s-SMEDDS. In addition, the physical state of the incorporated CARV and morphological analysis of s-SMEDDS was investigated by DSC, XRD, Raman mapping, and SEM. A stability study was conducted, in which the content of CARV was investigated and degradation products were characterized with the original LC-MS method.

2. Experimental

2.1. Materials

Carvedilol as a model drug (CARV) and Pharmacoat® 606 (hydroxypropyl methylcellulose substitution type 2910) were provided by Krka, d.d., Novo mesto, Slovenia. Aerosil® 300 Pharma (silica) was obtained from Evonik Industries, Germany, and Florite® R (calcium silicate) from Tomita Pharmaceutical Co., Ltd., Japan. Kolliphor® RH 40 (PEG-40 Hydrogenated Castor Oil) and PEG 400 were obtained from Sigma Aldrich, United States. Capmul® MCM EP (a mono-diglyceride of medium chain fatty acids) was obtained from Abitec Corporation, United

States, and castor oil, Ph. Eur. Grade, from Caesar & Loretz GmbH, Germany. Neusilin® US2 (magnesium aluminometasilicate) was obtained from Fuji Chemical Industry Co. Ltd., Japan. Syloid® 244FP and Syloid® XDP 3050 (silicas) were obtained from Grace GmbH & Co. KG, Germany.

Water was purified by reverse osmosis. Other chemicals were of HPLC or analytical grade.

2.2. Preparation of CARV-SMEDDS and spray drying dispersion

Liquid SMEDDS were developed in our previous study (Mandić et al., 2019). Oils (10% Capmul® MCM EP, 10% castor oil), surfactant (40% Kolliphor® RH 40), and co-solvent (40% PEG 400) were weighed into a glass beaker, heated to 60 °C, and homogenized on a magnetic stirrer. CARV was added to the mixture in a concentration of 100 mg per 1 g of SMEDDS and stirred at 50–60 °C until it was completely dissolved.

For preparation of the SD feed dispersion, a precise amount of CARV-loaded SMEDDS and a selected porous carrier—Aerosil® 300 Pharma, Florite® R, Neusilin® US2, Syloid® 244FP, or Syloid® XDP 3050 (with characteristics presented in Table 1)—were weighed in an Erlenmeyer flask in SMEDDS:carrier ratios of 1:1 (10 g + 10 g), 1.5:1 (15 g + 10 g), or 2:1 (10 g + 5 g) and suspended in 100 g of purified water. The SD feed dispersion was mixed on a magnetic stirrer for 2 h, 5 h, 24 h, or 48 h.

2.3. Solidification of SMEDDS

2.3.1. Spray drying

S-SMEDDS were produced by a Büchi Mini Spray Dryer B-290 with a two-fluid nozzle (inner diameter 0.7 mm and outer diameter 1.4 mm). The drying conditions were as follows: aspiration rate set to 100% (=drying gas flow rate of 35 m³/h), feed flow rate of 3.0 to 3.3 ml/min (using a peristaltic pump), inlet air temperature 130–140 °C, outlet air temperature 60–61 °C, nozzle cleaner 3 pulses per min, and rotameter height 50 mm (=atomization gas flow rate 0.601 m³/h). The SD feed dispersion was continuously stirred on a magnetic stirrer during the process.

The product was collected from the cyclone and the product collecting vessel underneath, weighed separately, and then joined into one sample. The process yield (η) was calculated by Eq. (1):

$$\eta = (\text{mass}_{\text{dry product}} / \text{mass}_{\text{dry entering substance}}) \times 100\% \quad (1)$$

The possibility of pre-filling the pores of the carrier Syloid® 244FP with drug-free SMEDDS or polymer HPMC (Pharmacoat® 606) was studied as a means of preventing irreversible adsorption of CARV-SMEDDS within the pores of the carrier and enhancing relative CARV content. SD feed dispersion composed of drug-free SMEDDS and carrier in a ratio of 0.5:1 (5 g + 10 g) was prepared in 100 g of water. With Pharmacoat® 606, first a 5% dispersion in 100 g of water was prepared, and afterward the carrier (10 g) was added to the polymer dispersion. The feed dispersion of the pore-filled carrier was spray dried after 1 day of mixing on a magnetic stirrer. The spray dried powders obtained were afterward used in the preparation of an aqueous dispersion with CARV-SMEDDS in a ratio of 1:1.5 (10 g of pore-filled carrier + 15 g of CARV-loaded SMEDDS in 100 g of purified water) and again spray dried after 1 day of dispersion mixing time.

2.3.2. Adsorption method

S-SMEDDS were also produced with the simple adsorption method (ADS) by mortar and pestle, with SMEDDS:carrier ratios of 1:1 and 2:1, to compare drug loading with SD products.

2.4. Loss on drying

The moisture content in s-SMEDDS and pure carriers was determined by thermogravimetric analysis (Mettler PM480 Delta Range, Mettler

Table 1

Comparison of particulate properties of the solid carriers Aeroperl® 300 Pharma, Florite® R, Neusilin® US2, Syloid® 244FP, and Syloid® XDP 3050.

Carrier	Average particle size (µm)	Average pore diameter (nm)	Average pore volume (cm ³ /g)	Specific surface area (m ² /g)	Lipid adsorption capacity	Bulk density (g/l)
Syloid® 244FP ^a , disordered mesoporous silica with intra-particle porosity	3.3	16–20	1.6	300	300 g/100 g	60
Neusilin® US2 ^b , disordered mesoporous aluminum magnesium silicate (granules) with wide pore size distribution	60–120	15 (5 nm – 3 µm)	1.16	300	320 ml/100 g	150
Aeroperl® 300 ^c , disordered meso- and macroporous silica (granulate) with inter-particle porosity	30–40	30	1.5–1.9	300	–	260
Florite® R ^d , disordered macroporous calcium silicate with deep and large pores	30	150	–	100	460 ml/100 g	70
Syloid® 3050 XDP ^e , disordered mesoporous silica with intra-particle porosity	50	21	1.7	320	300 g/100 g	275

^a Tan et al., 2013; W. R. Grace & Co.-Conn., Technical Note 09/15.

^b Fuji Chemical Industry Co., Ltd., 2007. Technical Newsletter; Gumaste et al., 2017.

^c Adler, 2017; Aerosil, Evonik; AEROSIL® and AEROPERL® Colloidal Silicon Dioxide for Pharmaceuticals Technical Information TI 1281; AEROPERL® 300 Pharma, Technical information 1414; Wang et al., 2014

^d Adler, 2017; Florite, (n.d.) Tomita Pharmaceutical Co., Ltd.

^e Adler, 2017; W. R. Grace & Co.-Conn., Technical Note 09/15.

Toledo, Switzerland). Three grams of sample was evenly placed on an aluminum pan and dried for 15 min at 85 °C. Two measurements were made.

2.5. Contact angle measurements

The contact angle of water was measured using the sessile drop method on a KRÜSS DSA100 Drop Shape Analyzer (Germany). Compacts of the selected carriers (Florite® R, Neusilin® US2, and Syloid® 244FP) and s-SMEDDS (Florite® R 1:1 and 2:1, Neusilin® US2 1:1 and Syloid® 244FP 1:1 and 2:1) were made using a manual hydraulic press. Aeroperl® 300 and s-SMEDDS produced with this carrier were excluded from contact angle measurements because they could not be compressed into compacts. A pressure of 369 MPa was applied to eliminate the impact of the carriers' particle size and porosity on the contact angle. SD products exhibited poor compaction properties, and leaking of SMEDDS from the compression tools was observed in most cases. Due to the compression force, migration of the liquid phase from the surface of the s-SMEDDS particles onto the surface of the compact occurred. Thus a smaller compression pressure of 74 MPa had to be used to compress products with higher SMEDDS loading and also for the Syloid® 244FP product with ratio of 1:1; however, compression of Neusilin® US2 2:1 was still not possible.

Three measurements of the contact angle were made for each sample and displayed as an average value.

2.6. Scanning electron microscopy (SEM)

The morphology of s-SMEDDS and corresponding carriers was observed by scanning electron microscopy (SEM) (Supra 35 VP, Carl Zeiss, Germany) at 1000× magnification, operating at 1 kV accelerating voltage.

2.7. Carvedilol content

The CARV content in the s-SMEDDS produced was determined using the previously described HPLC method (Mandić et al., 2019). Briefly, 10 µl of sample solution was injected into an HPLC system (Waters Alliance, Waters Corporation, USA) equipped with a Symmetry C18 column (250 mm length, 4.6 mm diameter, and 5 µm particle size), heated to 30 °C. The mobile phase was composed of methanol, buffer (4.5 g KH₂PO₄ and 0.61 g K₂HPO₄ per 1,000 ml of purified water), and acetic acid in a ratio of 60:40:0.3 (v/v/v). The detection wavelength was set to 284 nm. Sample and standard stock solutions were prepared in the mobile phase in a concentration of 500 µg/ml. The sample solutions were centrifuged, and then the supernatant of the sample solutions and standard stock solution were diluted 10 times to obtain sample and standard working solutions, respectively. The content of CARV was calculated with external standard calibration and expressed in mg per g of solid product.

Relative CARV content was calculated by Eq. (2):

$$\text{Relative CARV content (\%)} = \left(\frac{\text{determined CARV content}}{\text{theoretical CARV content}} \right) \times 100\% \quad (2)$$

Theoretical content of CARV in the samples was calculated by Eq. (3):

$$\text{CARV content (mg/g)} = \frac{(0,0909 \times \text{mass}_{\text{SMEDDS}} \times \eta)}{(\text{mass}_{\text{dry product}} \times 100\%)} \quad (3)$$

0,0909 share (w/w) of CARV in the liquid SMEDDS formulation (100 mg/1100 mg)

$\text{mass}_{\text{SMEDDS}}$ mass of SMEDDS, which was spray dried with the SD dispersion (mg)

η process yield (%)

$\text{mass}_{\text{dry product}}$ mass of dry product (s-SMEDDS) collected from the cyclone and the product collecting vessel

2.8. Thermal analysis

The differential scanning calorimetry analyses (DSC) of s-SMEDDS were performed with a differential scanning calorimeter (DSC1 STARe System, Mettler Toledo). The samples of s-SMEDDS (3–7 mg) were heated in an aluminum pan with a perforated lid from 0 to 160 °C at a scanning rate of 10 °C/min under the flow of nitrogen gas of 50 ml/min. An empty pan was used as a reference. The output data were evaluated by StarE 9.10 software.

2.9. X-ray diffraction studies (XRD)

The X-ray diffractograms were obtained by an PANalytical PW3040 / 60 X'Pert PRO diffractometer (CuK α 1 radiation, $\lambda = 1.5406 \text{ \AA}$) using the continuous scanning mode in the 2θ range from 3 to 32° and a step of 0.033° per 250 s to verify the crystallinity of the drug in the s-SMEDDS produced.

2.10. Raman spectroscopy

Spectroscopic analysis of the SD product (Syloid® 244FP product 2:1), crystalline and amorphous CARV, was performed by Raman line mapping using a WITec Alpha 500 Raman microscope (WITec, Germany), using a 532 nm laser with a power of 30 mW and a 20 \times confocal objective (ZEISS Microscope, Germany). The integration time was set to 0.1 s per spectrum. The surface analyzed was 250 $\mu\text{m} \times 1,000 \mu\text{m}$, with a step size in the x- and y-axes of 1.7 μm . All Raman spectra were acquired in the spectral range of 3,600 to 100 cm^{-1} . All the data were acquired and manipulated by WITec software (WITecProject 5.2 and WITecControl 5.2).

2.11. Preparation of amorphous CARV

Crystalline CARV was melted in a platinum pot on a hotplate at approximately 130 °C. The melted substance was immediately cooled on an ice bath, forming a solidified melt. It was stored in a desiccator until the analysis.

2.12. Determination of self-emulsifying properties

To assess the redispersion time, 1 g of s-SMEDDS was transferred into a 250 ml Erlenmeyer flask. While stirring at 200 rpm, 250 ml of water was added and the time to achieve complete redispersion was measured, which was visually assessed as the formation of a transparent dispersion.

To evaluate the self-microemulsifying properties, the dispersion of 1 g of s-SMEDDS in 250 ml of water, a 0.1 M hydrochloric acid solution with a pH of 1.2, or a phosphate buffer solution with a pH of 6.8 was prepared and stirred at room temperature for 30 min at 200 rpm on a magnetic stirrer, allowing complete redispersion. Afterward it was filtered through a 0.45 μm membrane filter (regenerated cellulose) to remove undissolved particles of excipients (carriers). The droplet size of the filtered dispersion was measured by photon correlation spectroscopy (PCS) at 25 °C with the Zetasizer Nano Series (Malvern Instruments Ltd., United Kingdom). Measurements were repeated in triplicate, and the calculated average values were used.

2.13. Dissolution studies

In vitro dissolution testing was performed using a USP Apparatus 2 (Vankel VK 7010, Vankel industries, USA and Agilent 708-DS, Agilent Industries, USA). A precisely weighed amount of s-SMEDDS, containing approximately 25 mg of CARV, was transferred into 900 ml of dissolution media (diluted hydrochloric acid pH 1.2 or phosphate buffer pH 6.8) with a temperature of 37 °C \pm 0.5 °C. The paddle speed was set to 50 rpm. As a reference, 25 mg of pure CARV and liquid SMEDDS corresponding to 25 mg of CARV were tested. At predetermined time

intervals of 10, 20, 30, 45, 60, and 120 min with 15 min of final spin at 200 rpm (infinity spin), samples were collected (5 ml), filtered through a 0.45 μm pore membrane filter (regenerated cellulose), and analyzed using the HPLC method described in Section 2.7. Standard stock solution was diluted with dissolution media to obtain a working standard solution at a concentration of 25 $\mu\text{g}/\text{ml}$. The cumulative percentage of dissolved CARV was calculated regarding the determined content and plotted versus time.

2.14. Liquid chromatography–mass spectrometry (LC-MS)

The LC-MS analyses were carried out on a Thermo Fisher Scientific Vanquish UHPLC System (San Jose, USA) coupled with a Thermo Fisher Scientific Q Exactive Focus mass spectrometry system using an electrospray ionization (ESI) interface. For chromatographic separation, a Waters Corporation (Milford, USA) Symmetry C18 column (250 mm \times 4.6 mm, 5 μm particle size) was used throughout the analysis; the column temperature was set to 30 °C. When preparing various mobile phases, a 0.01 mol/l ammonium acetate buffer with the pH adjusted to 4.5 with acetic acid was used. Sample solutions were prepared the same way as for CARV content determination, with the exception of final dilution with the mobile phase (see Section 2.7). The approximate content of individual impurities was evaluated by comparing peak areas.

The initial isocratic elution for screening known related substances was performed using a mixture of ammonium acetate buffer (pH = 4.5), methanol, and acetic acid in a 40:60:0.3 (v/v/v) ratio at a constant flow of 1.0 ml/min. The sample injection volume was 5 μl . The analysis time for a single run was 45 min. To analyze delayed peaks that do not elute from the column during isocratic elution, a gradient elution was carried out with the ammonium buffer solution (pH = 4.5) used as Mobile Phase A and acetonitrile as Mobile Phase B. The gradient consisted of 0 to 5 min at 10% B, a linear increase to 90% B from 5 to 30 min, isocratic elution at 90% B from 30 to 44 min, a return to starting conditions from 44 to 45 min, and finally equilibration at starting conditions until 50 min (end of run).

The mass spectrometer ESI(+) ion source conditions were set as followed: spray voltage = 3,500 V, capillary temperature = 300 °C, sheath gas = 65, auxiliary gas = 20, sweep gas = 1, and S-Lens RF Level = 55. The probe heater temperature was set to 400 °C. The fragmentation of parent ions was achieved using collision-induced dissociation (HCD) with an isolation window of 2.0 m/z and a normalized collision energy (NCE) of 30.0 eV.

2.15. Stability study and determination of amide impurities

The samples submitted to the stability study were stored at 20–25 °C and < 60% relative air humidity in a container, which was sealed in aluminum foil. For evaluation of CARV content and the increase in amide formation during the stability study, conditions of the HPLC method (Section 2.7) were modified in accordance with the chromatographic conditions of the LC-MS method (Section 2.14): gradient instead of isocratic elution, run time 50 min, and wavelength of detection 244 nm. With these chromatographic conditions, the same results of amide content as in the LC-MS method were obtained by comparing peak areas. CARV content was determined by comparing the peak area with a standard solution of known CARV concentration.

3. Results and discussion

3.1. Production of solid SMEDDS with spray drying

With the aim of producing solid SMEDDS with high drug loading and acceptable flow properties, various porous carriers with high liquid loading capacity were used: Aeroperl® 300 Pharma, Florite® R, Neusilin® US2, Syloid® 244FP, or Syloid® XDP 3050 (Table 1). Process parameters were adjusted to obtain a high process yield. The SD feed

dispersion was mixed for 2 h, 5 h, 24 h, or 48 h, and the impact of mixing time (i.e., contact time of water dispersion of SMEDDS with the carrier) on the process yield was studied.

CARV-SMEDDS was loaded in three different SMEDDS:carrier ratios (1:1, 1.5:1, and 2:1), and the differences in the process yield were studied. For simplification of the text, all products are referred with the carrier name (or its abbreviation) and the ratio, which refers to the SMEDDS:carrier ratio (e.g. Syloid® 244FP 2:1 short for SMEDDS:Syloid® 244FP = 2:1).

3.1.1. Adjustment of spray drying process parameters

Initial experiments were performed with Syloid® 244FP in ratios of 1:1 and 2:1, using the following experimental conditions: feed flow rate of 4.5 ml/min, drying gas flow rate of 35 m³/h, inlet temperature of 120 °C, outlet air temperature of 45 to 50 °C, and atomization gas flow rate of 0.473 m³/h. Sticking of the particles on the walls of the drying chamber and large amount of particles on the bottom of the drying chamber, instead of in the collecting chamber, was observed. Due to the low outlet air temperature (45–50 °C), insufficient drying of the particles was presumed as a reason for particle adhesion. Therefore, the feed flow rate was decreased to 3.3 ml/min and the inlet air temperature increased to 130 to 140 °C, which resulted in an increased outlet air temperature (59–61 °C), lower adhesion of the particles to the chamber walls, and increased amount of the product in the cyclone and the collecting chamber, all of which together increased the process yield. Nonetheless, a considerable amount of the product was collected in the vessel on the bottom of the chamber, where larger and heavier particles are eliminated, because they cannot pass into the cyclone with the drying gas flow. Therefore, to produce smaller droplets of dispersion, the atomization gas flow rate was increased to 0.601 m³/h. This change resulted in a 19% higher process yield (66.0 vs. 84.9% with Syloid® 244FP 2:1). In a study by Čerpnjak et al. (2015b), it was shown that a higher atomization pressure results in a lower mean droplet size after reconstitution of the s-SMEDDS produced, which is a crucial benefit for preserving the advantages of the drug incorporated into the SMEDDS. Thus, in all further experiments, the atomization gas flow rate was set to 0.601 m³/h and the drying gas flow rate to 35 m³/h, and the outlet air temperature was maintained between 60 and 61 °C by regulating the feed flow rate and inlet air temperature. The initial and optimized SD conditions are presented in Table 2.

3.1.2. Influence of dispersion composition and mixing time on process yield

In addition to the process parameters, the process yield was also strongly affected by the choice of the carrier and the time of its contact

Table 2
Starting and optimized spray drying process parameters.

Process parameters	Initial	Optimized
Drying gas flow rate	35 m ³ /h (maximum)	35 m ³ /h (maximum)
Feed flow rate	4.5 ml/min	3.0–3.3 ml/min
Inlet air temperature	120 °C	130–140 °C
Atomization gas flow rate	0.473 m ³ /h	0.601 m ³ /h

Table 3
Impact of different mixing time of spray drying dispersion on process yield.

SMEDDS:carrier ratio	Dispersion mixing time	Process yield (%)				
		Neusilin® US2	Syloid® 244FP	Syloid® 3050 XDP	Aeroperl® 300	Florite® R
1:1	2 h	66.4	67.2	55.6	62.6	65.1
1:1	24 h	84.4	67.9	–	75.2	78.8
1:1	48 h	83.5	78.5	–	–	–
1.5:1	24 h	73.8	75.8	–	77.4	75.5
1.5:1	48 h	85.1	84.1	–	–	–
2:1	2 h	60.2	67.2	56.5	68.0	73.8
2:1	24 h	78.8	83.0	–	77.1	81.8
2:1	48 h	84.4	–	–	–	–

with the aqueous dispersion of SMEDDS; that is, the mixing time of the SD dispersion.

The dependence of the SD process yield on the type of carrier and SMEDDS:carrier ratio is presented in Table 3. Differences in the process yield cannot be attributed to the chemical composition of the carriers, since Syloid® 244FP, Aeroperl® 300 and Syloid® 3050 XDP are all silicas, however the performance of the Syloid® 3050 XDP was inferior to the other two carriers and was therefore omitted from further studies. The carriers differ in pore length and volume, depending on the size of the particles. Hence, the time needed to fill the microemulsion in the particle pores is expected to be affected by the size of the particles (Choudhari et al., 2014). Among the tested carriers Syloid® 244FP has the smallest particle size (only 3 µm), whereas Florite® R differs from the others due to the bigger average pore diameter (150 nm) and much lower specific surface area (100 m²/g) (Table 1). Both also have considerably lower bulk density compared to the other carriers. Despite different characteristics, no considerable difference in process yield values was observed among the carriers (with the exception of Syloid® 3050 XDP). Nonetheless, at the lowest SMEDDS:carrier ratio (1:1) the impact of carrier's particle size on the process yield was observed, since the carriers with largest (Neusilin® US2) and smallest particles (Syloid® 244FP) resulted in the highest (84%) and the lowest process yield (68%) upon 24 h dispersion mixing time, respectively. Namely, 3 µm sized particles of Syloid® 244FP can be lost through the filters with the drying air flow. On the other hand, their small size is linked with the shortest pore length, which contributed to the fastest absorption of microemulsion, as seen from highest process yield (determined at 2 h mixing time of SD dispersion) and comparable amount of SMEDDS loaded upon 2 h or 24 h of contact time between the microemulsion and the carrier. In keeping with this, slower SMEDDS adsorption was noticed for Neusilin® US2, which could be linked to its bottle-neck shaped pores as proposed previously (Choudhari et al., 2014). Although most pronounced in Neusilin® US2, prolonged mixing time of SD dispersion resulted in an increased process yield also for other carriers, with the highest process yields obtained upon 48 h of dispersion mixing time. Prolonged contact time between porous carriers and dispersion of SMEDDS allows more efficient adsorption of SMEDDS into the pores of the carrier, and therefore a lower amount of unabsorbed SMEDDS could be lost by adsorption on the filters or passing through the filters during the SD process. In addition, adsorption of the surfactants present in the SMEDDS onto the surface of the carrier's pores modifies its surface and ease further penetration of SMEDDS into the pores while the water is removed during SD. With more SMEDDS distributed in the pores instead on the surface of the carrier, the particles had a lower tendency to stick to the walls of the SD chamber and were thus transported into the cyclone with the drying gas, where the final product was collected. Nevertheless, in addition to the overall prolonged time of solid SMEDDS production, prolonged SD mixing time is also associated with a greater risk of incomplete drug desorption from the carrier. Therefore, 24 h was selected as an optimal mixing time for the preparation of SD dispersion.

The influence of SMEDDS:carrier ratio on the SD process yield was most pronounced for the Syloid® 244FP carrier, which has significantly smaller particles than the other carriers. Positive correlation between

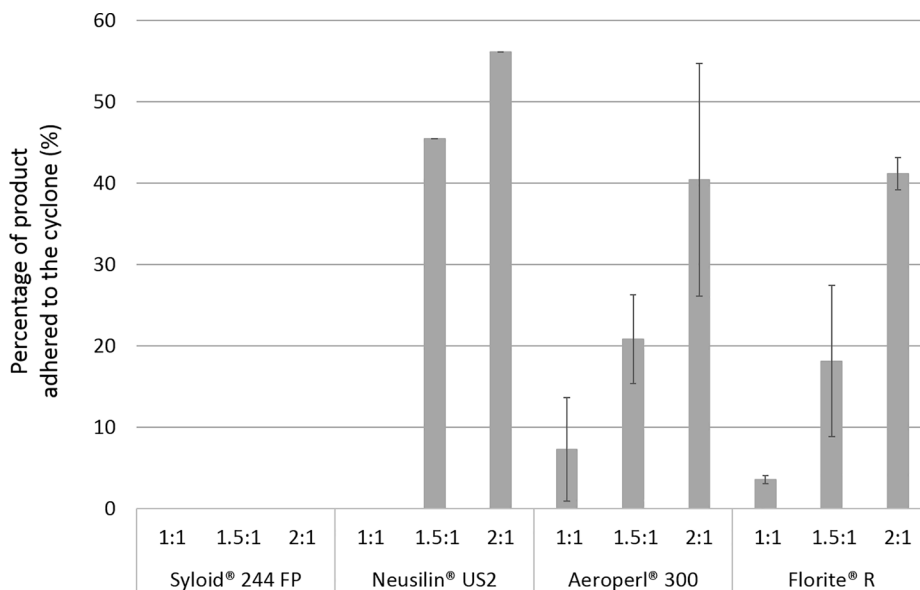


Fig. 1. Percentage of dried particles adhered to the cyclone wall in s-SMEDDS with different SMEDDS:carrier ratio. (Note: SD dispersion was stirred for 24 h prior to the solidification process).

the process yield and higher SMEDDS:carrier ratio can be attributed to the lower extent of particle loss through the filters with the drying air flow when loaded with a larger amount of SMEDDS. Namely, high SMEDDS-loaded particles are presumably heavier, which is beneficial for their separation from the drying air flow in the cyclone. An increased fraction of dried particles adhering to the cyclone wall was observed with the increase in the SMEDDS:carrier ratio in the products, with the exception of Syloid® 244FP-based products, which showed no sticking to the cyclone wall (Fig. 1). In keeping with this, Syloid® 244FP with its smallest particles and, alternatively, Florite® R with its large and deep pores could be selected as the most perspective carriers for converting SD dispersion with the highest SMEDDS:carrier ratio into s-SMEDDS, due to the highest process yields obtained at SMEDDS:carrier ratio 2:1 (after 24 h mixing time of SD dispersion).

3.2. Characterization of solid SMEDDS

3.2.1. CARV content

The determined and relative contents (determined drug content expressed relative to the theoretical content; see Eq. (2)) of CARV were

compared for products with SMEDDS:carrier ratios of 1:1, 1.5:1, and 2:1, which were obtained with the SD method and for s-SMEDDS produced with the ADS method (i.e., as a method with minimal substance loss). Because no significant differences in CARV content were observed in SD products with the same composition and different mixing time of SD dispersion (data not shown), s-SMEDDS obtained after 24 h mixing time of SD dispersions were chosen for further evaluation.

As shown in Table 4, a higher SMEDDS:carrier ratio commonly results in higher CARV content. Aeroperl® 300 and Neusilin® US2 allowed production of s-SMEDDS with the highest CARV content at a SMEDDS:carrier ratio of 2:1 (58.7 mg/g and 55.8 mg/g, respectively), whereas lower CARV content was obtained with Florite® R and Syloid® 244FP (53.8 mg/g and 51.2 mg/g, respectively). Relative content ranged from 83 to 97% (Table 4), and more than 85% of CARV content was obtained with all carriers, with the exception of Syloid® 244FP at the highest SMEDDS:carrier ratio (2:1). For SD technology, these values of relative content can be considered relatively high because some drug loss is normally expected in the SD process. Nonetheless, it is interesting to note that at the highest SMEDDS:carrier ratio (2:1) the lowest CARV content was determined for the Syloid® 244FP product, which was

Table 4

CARV content in s-SMEDDS (mg of CARV per g of product) produced with the SD (24 h of dispersion mixing time) and ADS method.

Carrier	SMEDDS:carrier	Spray drying		Adsorption	
		Content (mg/g)	Relative content (%)	Content (mg/g)	Relative content (%)
Neusilin® US2	1:1	42.9	92.1	45.0	95.0
	1.5:1	49.0	88.1	–	–
	2:1	55.8	90.7	60.0	96.5
Syloid® 244FP	1:1	47.5	102.2	44.0	94.2
	1.5:1	51.1	92.6	–	–
	2:1	51.2	83.3	58.9	95.7
Syloid® 3050 XDP	1:1	40.9	88.7	–	–
	2:1	51.7	84.5	–	–
Aeroperl® 300	1:1	43.3	94.5	45.0	97.3
	1.5:1	51.9	94.7	–	–
	2:1	58.7	96.5	58.2	95.1
Florite® R	1:1	44.0	95.4	43.7	93.6
	1.5:1	49.2	89.3	–	–
	2:1	53.8	88.2	58.3	94.8

identified as the best carrier regarding the process yield (see Table 3) and was the only one for which the product at the highest SMEDDS:carrier ratio did not adhere to the cyclone wall (see Fig. 1). A possible explanation for lower drug content is incomplete desorption of CARV-loaded SMEDDS from the pores of the carrier, which is also in agreement with the incomplete drug release from Syloid® 244FP and Florite® R-based products (see Figs. 4 and 5). According to Gumaste et al. (2017), complete drug release could be obtained upon blocking the deepest pores of the carrier with a suitable excipient. In line with this study, we aimed to partially prefill the pores of Syloid® 244FP with either unloaded SMEDDS (i.e., CARV-free SMEDDS) or HPMC solution. Water dispersion of the pore-filling agent and the carrier at ratio 0.5:1 was stirred for 24 h prior to the SD process. The pore-filled carriers obtained were further used for production of s-SMEDDS at a SMEDDS:carrier ratio of 1.5:1. In both products obtained, the CARV content in obtained product was even lower than with untreated carrier (29.9 mg/g or 62% of theoretical CARV content for the product with SMEDDS-prefilled pores, and 28.7 mg/g or 61% of theoretical CARV content for HPMC-prefilled pores). We presume that, during mixing of the SD dispersion, SMEDDS or polymer adsorbed onto the surface of the carrier first, rather than entering into the pores, or possibly even obstructed the openings of the pores, resulting in lower capacity of the carrier for further SMEDDS loading. The phenomenon of SMEDDS covering the surface of the carrier already at a low concentration of SMEDDS was confirmed in SEM and contact angle measurements (see Sections 3.2.2 and 3.2.3).

Another possible explanation for lower CARV content can be disproportional loss of non-incorporated CARV-loaded SMEDDS (in comparison to the loss of carrier) from the SD dispersion during the drying process due to the exceeding SMEDDS loading capacity of Syloid® 244FP. Similar explanation can be proposed for the carrier Florite® R. Although the manufacturer states that Florite® R can absorb an amount of liquid fivefold its own weight (Florite, (n.d.) Tomita Pharmaceutical Co., Ltd.), it is possible that higher SMEDDS loading in our case was prevented because the carrier was mixed with o/w

microemulsion and not with lipids only, which is the method for determining lipid adsorption capacity by the manufacturer.

Despite having similar specification characteristics with regard to lipid adsorption capacity, the carriers behaved differently during the SD process, whereas products obtained by the simple adsorption method have more comparable CARV content (Table 4). In the adsorption method, the carrier is blended with pure liquid SMEDDS, and minimal loss of SMEDDS is expected if the lipid adsorption capacity of the carrier is not exceeded. On the other hand, in the SD method the carrier is mixed with a water dispersion of SMEDDS prior to SD to allow penetration and adsorption of o/w microemulsion droplets. Considering the fact that the carriers have different pore size, length and shape, some SMEDDS droplets remain dispersed in the water and some precipitation of drug in the SD dispersion can occur, therefore some loss of SMEDDS and drug is expected during the SD process. CARV-SMEDDS loading on Aeroperl® 300 and Neusilin® US2 was less affected by the solidification method applied. A possible explanation is that their particles with a high specific surface area and wide pore size distribution with meso- and macropores, according to the manufacturers' data, were more readily loaded either with SMEDDS or with oil-in-water microemulsion formed in SD dispersion.

3.2.2. Surface morphology of granulates and physical state of carvedilol

The particle morphology of all products with different SMEDDS:carrier ratios was studied using SEM. From SEM microphotographs (Fig. 2), it is obvious that the solidification procedure affected the shape and size of the particles. The spherical and porous particles of Neusilin® US2 carrier were already changed to a certain degree after SD with SMEDDS at the lowest ratio tested (i.e., 1:1), which was attributed to the exposure of high pressure when sprayed through the nozzle. The porosity of the particles can still be observed; however, partial loading of SMEDDS on the surface of the particles is seen. With increasing SMEDDS concentration in the formulation, an absence of spherical particles can be observed and the presence of smaller particles and their agglomerates

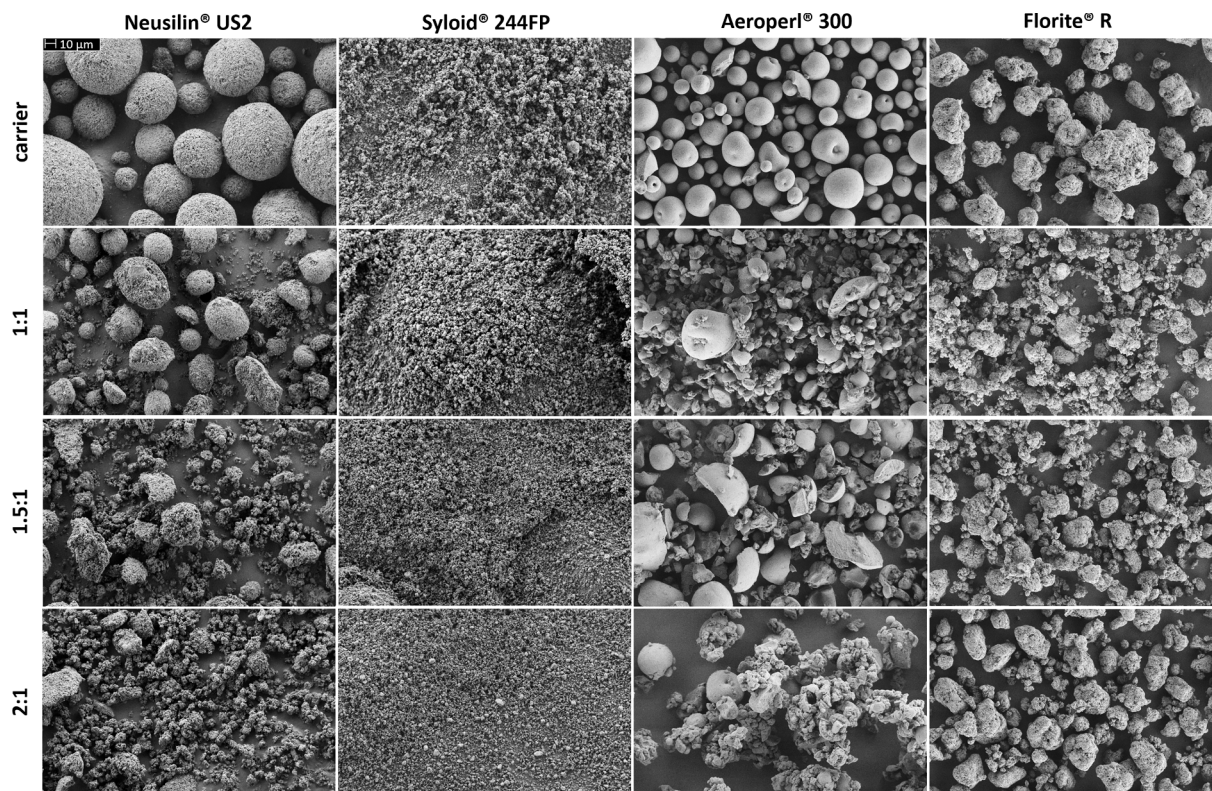


Fig. 2. SEM images of the carriers and s-SMEDDS under 1000× magnification.

of irregular shapes and various size. Presumably, higher amount of SMEDDS adsorbed on the surface of the carrier particles allowed adhesion of the particles into agglomerates. Due to their irregular shape and size, poor flow properties of Neusilin® products are expected. A similar effect was also observed for Aeroperl® 300 because SEM images show a transformation of its spherical particles into smaller irregularly shaped particles already at a SMEDDS:carrier ratio of 1:1, whereas larger agglomerates were formed at a ratio of 2:1.

In contrast to Neusilin® US2 and Aeroperl® 300, particles of the pure carriers Syloid® 244FP and Florite® R are irregularly shaped, with Syloid® 244FP particles being significantly smaller in comparison with the other carriers. For Syloid® 244FP-based products, formation of particle agglomerates can already be observed at the lowest SMEDDS:carrier ratio. With the increasing share of SMEDDS, larger particles were obtained with many voids within the agglomerated particles. On the other hand, no significant change in particle shape was observed with SD Florite® R-based products compared to the pure carrier. Fragmented particles were agglomerated with larger particles, and, except for larger size, no other visual difference can be attributed to the Florite® R-based products with a higher ratio of SMEDDS because the products had an irregular shape with wide particle size distribution and a visibly rough surface at all SMEDDS:carrier ratios tested.

The physical state of CARV in s-SMEDDS was first studied by DSC. No thermal events were observed on the DSC heating curves of SD products, in contrast to crystalline CARV, with a melting point at 115.6 °C (data not shown). Due to the observed slower and incomplete drug release from Syloid® 244FP and Florite® R products (see Section 3.2.3), we have assumed that CARV was present in a crystalline form in s-SMEDDS. The results of XRD and Raman spectroscopy (presented in Fig. 3 and S1, respectively) have shown that solidification of liquid SMEDDS by SD does not cause crystallization of the incorporated drug. As can be seen in Fig. 3, which shows diffractograms of pure crystalline and amorphous drug and s-SMEDDS with Syloid® 244FP, no sharp diffraction lines of crystalline CARV at a 2θ from 11° to 30° were observed in SD products. A sample of the Syloid® 244FP product 2:1 was also studied with Raman mapping. The Raman spectra were homogenous throughout the entire surface analyzed and were a combination of responses of CARV and the carrier. The Raman spectra of s-SMEDDS were also compared with crystalline and amorphous CARV (Fig. S1). The amorphous form had some wider or shifted Raman bands when compared to the crystalline form of CARV. In s-SMEDDS many bands characteristic of CARV were covered with wide and highly intensive bands of the carrier;

nevertheless, a band at 1,288 cm⁻¹ was observed in all three samples (s-SMEDDS and both physical forms of CARV), indicating the presence of CARV on the surface of the s-SMEDDS. In addition, a band at 1,630 cm⁻¹ was observed in amorphous CARV and in s-SMEDDS, whereas in crystalline CARV it was shifted to 1,635 cm⁻¹.

3.2.3. Wettability, self-emulsifying properties, and dissolution results

Contact angle measurements were made to inspect the wetting properties of the s-SMEDDS in comparison to the pure carriers of Florite® R, Neusilin® US2, and Syloid® 244FP. We aimed to investigate, whether higher SMEDDS:carrier ratio resulted in more extensive adsorption of SMEDDS at the surface of carriers and thus in lower contact angle.

The contact angle was measured at different time points, and a decrease in the contact angle with time was observed for all compacts due to the penetration of liquid into the pores of the compacts and also due to the dissolution of SMEDDS in the droplet of water. The results of contact angle measurements at a time point of 0 s are therefore shown in Table 5. When comparing materials that were compressed with the same pressure, it can be observed that the contact angle with Neusilin® US2 and Florite® R-based products with ratio 1:1 was smaller than with the pure carrier. In case of Syloid® 244-based products smaller contact angle was detected on s-SMEDDS with higher SMEDDS loading, which altogether indicates the adsorption of SMEDDS on the surface of the carriers even at the lowest SMEDDS:carrier ratio.

Table 5

Contact angle of water with solid carriers and spray dried s-SMEDDS (information on the compression pressure is given in parentheses) at the time point of 0 s.

Sample and compaction pressure	Contact angle
Florite® R (369 MPa)	21.7°
SMEDDS:Florite® R = 1:1 (369 MPa)	13.9°
SMEDDS:Florite® R = 2:1 (74 MPa)	16.6°
Neusilin® US2 (369 MPa)	23.2°
SMEDDS:Neusilin® US2 = 1:1 (369 MPa)	16.2°
*Syloid® 244FP (74 MPa)	0°
SMEDDS:Syloid® 244FP = 1:1 (74 MPa)	14.7°
SMEDDS:Syloid® 244FP = 2:1 (74 MPa)	13.0°

* With neat Syloid® 244®FP immediate penetration of water was observed, which indicates porosity of the compact, therefore it cannot be taken into consideration for comparison with the other products.

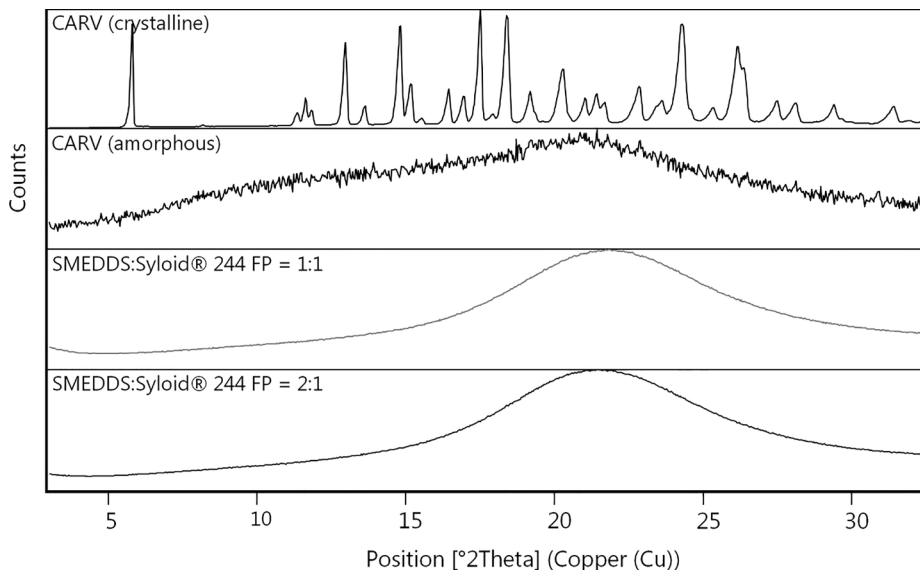


Fig. 3. XRD diffractograms of crystalline CARV, amorphous CARV and Syloid® 244FP products at SMEDDS:carrier ratio 1:1 and 2:1.

Table 6

Droplet size of (s-)SMEDDS and redispersion time in water.

Sample and SMEDDS:carrier ratio		Z-average diameter (nm)	PDI (\pm SD)	Peak 1 (nm)	Peak 2 (nm)	Peak 3 (nm)	Redispersion time
SMEDDS		23.1 \pm 0.2	0.072 \pm 0.004	23.1	–	–	immediate
CARV-SMEDDS		81.6 \pm 1.2	0.458 \pm 0.001	22.3	149.4	–	immediate
Neusilin® US2	1:1	82.3 \pm 18.4	0.453 \pm 0.102	26.44	162.9	–	<50 s
	1.5:1	65.7 \pm 9.0	0.531 \pm 0.011	25.83	175.8	–	<40 s
	2:1	46.2 \pm 3.2	0.652 \pm 0.176	24.84	220.3	–	<20 s
Syloid® 244FP	1:2	200.6 \pm 29.0	0.379 \pm 0.028	278.8	4607	–	<50 s
	1:1	147.6 \pm 1.1	0.258 \pm 0.006	176.4	5551	–	<50 s
	1.5:1	122.5 \pm 3.0	0.422 \pm 0.045	23.64	197	4406	<50 s
	2:1	51.6 \pm 2.1	0.806 \pm 0.006	26.38	354.8	2304	<20 s
Aeroperl® 300	1:1	153.8 \pm 1.0	0.181 \pm 0.021	35.36	185.6	–	<180 s
	1.5:1	144.9 \pm 1.5	0.211 \pm 0.000	35.35	172.6	–	<180 s
	2:1	35.4 \pm 0.7	0.447 \pm 0.008	24.34	248.4	–	<60 s
Florite® R	1:1	115.3 \pm 5.0	0.387 \pm 0.011	167.6	4584	–	<60 s
	1.5:1	68.5 \pm 3.5	0.576 \pm 0.121	34.6	207.7	4848	<120 s
	2:1	45.0 \pm 0.5	0.301 \pm 0.009	61.9	125.8	–	<60 s

As expected SD products have good wetting properties, therefore a short redispersion time of s-SMEDDS is expected.

Preservation of self-microemulsifying properties after the SD solidification process was studied and the results are shown in Table 6. After redispersion of liquid SMEDDS in water, a monodisperse microemulsion was obtained, with a droplet size (Z-average value, Z-avg) of 23.1 nm and a low PDI (0.072). Aqueous dispersion of CARV-loaded SMEDDS was polydisperse (PDI 0.458) due to detection of two peaks: the first attributed to the droplets of microemulsion (22.3 nm), and the second to the nanoparticles of precipitated drug (149.4 nm), as reported in our previous study (Mandić et al., 2019). The redispersion time of liquid SMEDDS was immediate, as expected. Droplet size was comparable when either 0.25 g or 1 g of SMEDDS was redispersed in 250 ml of water, indicating that droplet size of aqueous dispersions of different s-SMEDDS can be directly compared despite differences in SMEDDS' content. Aqueous dispersion of all s-SMEDDS was polydisperse, in line with liquid CARV-SMEDDS. The smallest peak was attributed to droplets of microemulsion and a larger peak to nano- or microparticles of either precipitated CARV or smaller particles of the carrier, which were not removed by the filtration. In some samples, a larger peak in the micrometer range was observed, which can most likely be attributed to impurities during measurement (e.g., dust particles); nevertheless, this has no significance when studying SME properties.

Preservation of microemulsion droplet size (i.e. peak 1) was confirmed for all s-SMEDDS, with the exception of Syloid® 244FP and Florite® R-based products with SMEDDS:carrier ratio 1:1. A possible explanation is irreversible adsorption of surfactants to the carriers' surface, exhibiting bigger effect on emulsion formation in the products with lower SMEDDS loading (i.e. with lower SMEDDS:carrier ratio). This presumption was confirmed also by Syloid® 244FP-based product with SMEDDS:carrier ratio 1:2, which exhibited even larger droplet size after redispersion (279 nm vs. 176 nm observed at ratio 1:1). Nevertheless, all dispersions appeared translucent and could be visually assessed as microemulsions. The redispersion time of all s-SMEDDS was below 1 min, with the exception of Aeroperl® 300-based products that redispersed in up to 3 min. Products with SMEDDS:carrier ratio 2:1 exhibited the fastest redispersion time regardless of the carrier used, with only 20 s needed for Syloid® 244FP and Neusilin® US2 -based s-SMEDDS. The preservation of SME properties is in accordance with fast in vitro drug release.

The short redispersion time and the presence of drug in a molecularly dispersed form in s-SMEDDS allowed fast and complete drug release in vitro in acidic media, which was significantly higher than the dissolution of crystalline CARV (Table 7). In dissolution media with a pH of 1.2, all products released more than 80% of CARV within the first 10 min, with the exception of Syloid® 244FP 1:1, which released approximately 70%,

Table 7

Parameters of in vitro dissolution testing at a pH of 1.2 (% of CARV released in 10 min, 30 min, and maximum after infinity spin) and Z-average droplet size, expressed as an average value with a standard deviation.

Carrier	SMEDDS: carrier ratio	Q10min (%)	Q30min (%)	Qmax (%)	Z-avg (nm)
Syloid® 244FP	1:1	68 \pm 1	73 \pm 3	93 \pm 3	230.6 \pm 15.6
	1.5:1	87 \pm 3	90 \pm 3	94 \pm 2	180.3 \pm 3.6
	2:1	90 \pm 0	92 \pm 1	93 \pm 1	33.4 \pm 1.1
Neusilin® US2	1:1	94 \pm 3	97 \pm 1	99 \pm 0	36.0 \pm 1.4
	1.5:1	101 \pm 6	102 \pm 7	103 \pm 6	25.0 \pm 0.3
	2:1	101 \pm 4	103 \pm 4	104 \pm 4	24.6 \pm 0.8
Aeroperl® 300	1:1	83 \pm 5	86 \pm 5	93 \pm 3	92.8 \pm 0.9
	1.5:1	83 \pm 0	86 \pm 2	91 \pm 0	48.8 \pm 1.6
	2:1	95 \pm 1	97 \pm 0	100 \pm 1	44.4 \pm 2.0
Florite® R	1:1	83 \pm 2	90 \pm 1	95 \pm 1	181.1 \pm 9.5
	1.5:1	95 \pm 3	100 \pm 4	103 \pm 4	64.38 \pm 6.4
	2:1	90 \pm 2	93 \pm 3	94 \pm 3	26.1 \pm 1.3
Liquid CARV-loaded SMEDDS		98 \pm 2	99 \pm 1	99 \pm 1	19 \pm 0.2
CARV		48 \pm 4	59 \pm 4	75 \pm 1	–

whereas only approximately 50% of crystalline CARV was dissolved in the same time unit. Drug release was faster for 2:1 products, which is in line with the better-preserved SME properties (a smaller size of peak 1 and Z-avg) of products with larger amount of SMEDDS. In line with this, Neusilin® products exhibited the fastest drug release, which was also immediate for the 1:1 product (94% in 10 min). Fig. 4 presents the dissolution profiles of products with a ratio of 2:1 at a pH of 1.2, showing faster and more extensive drug release than pure drug, with more than 90% of drug released from all products.

In dissolution media with a pH of 6.8, which is more discriminative due to the lower solubility of CARV, all s-SMEDDS exhibited significantly faster drug release than crystalline CARV (Table 8). After the first 10 min, the amount of drug released from s-SMEDDS varied from 41% (Syloid® 244FP 1:1) to 103% (Neusilin® 2:1), whereas only 1% of

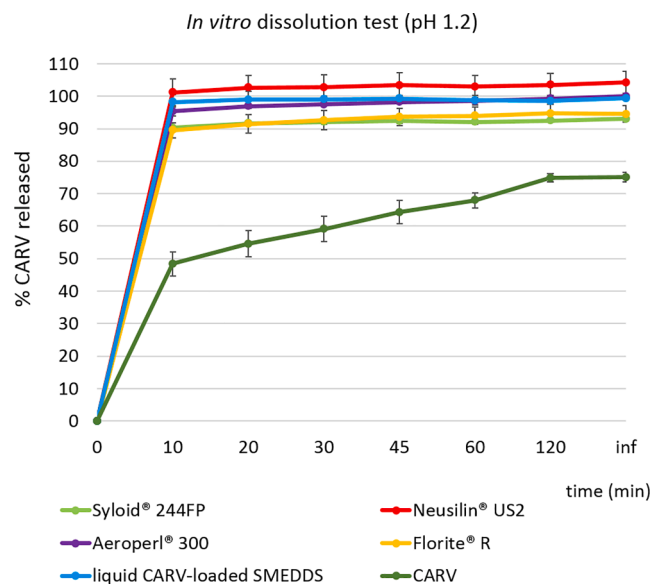


Fig. 4. *In vitro* carvedilol dissolution profiles from s-SMEDDS with SMEDDS: carrier ratio 2:1 compared to dissolution of the pure drug at pH 1.2.

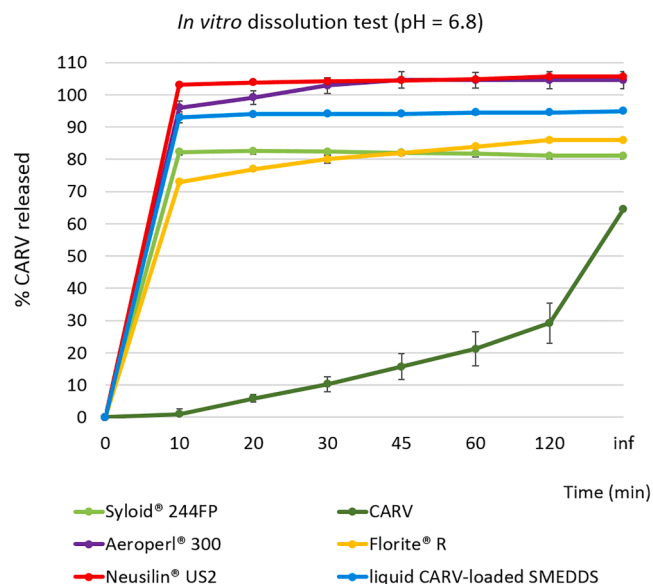


Fig. 5. *In vitro* carvedilol dissolution profiles from s-SMEDDS with SMEDDS: carrier ratio 2:1 compared to dissolution of the pure drug at pH 6.8.

Table 8

Parameters of *in vitro* dissolution testing at pH 6.8 (% of CARV released in 10 min, 30 min and maximum after infinity spin) and Z-average droplet size, expressed as an average value with a standard deviation.

Carrier	SMEDDS:carrier ratio	Q10min	Q30min	Qmax	Z-ave (nm)
Syloid® 244FP	1:1	41 ± 2	57 ± 3	96 ± 5	162.6 ± 0.1
	1.5:1	49 ± 2	65 ± 3	85 ± 4	184.6 ± 29.9
	2:1	82 ± 1	82 ± 0	82 ± 0	34.54 ± 0.2
Neusilin® US2	1:1	84 ± 2	89 ± 3	95.1 ± 4	39.2 ± 1.5
	1.5:1	80 ± 2	86 ± 2	107 ± 2	41.5 ± 7.1
	2:1	103 ± 1	104 ± 0	108 ± 0	27.8 ± 0.1
Aeroperl® 300	1:1	63 ± 5	73 ± 5	93 ± 1	230.7 ± 2.4
	1.5:1	77 ± 3	87 ± 1	99 ± 3	69.2 ± 0.2
	2:1	96 ± 2	103 ± 2	105 ± 3	65.0 ± 3.0
Florite® R	1:1	59 ± 2	64 ± 2	76 ± 2	187.1 ± 1.8
	1.5:1	73 ± 2	79 ± 3	88 ± 3	45.6 ± 2.2
	2:1	73 ± 1	80 ± 1	86 ± 2	34.9 ± 0.3
liquid CARV-loaded SMEDDS		93 ± 2	94 ± 0	94 ± 0	30.9 ± 0.0
CARV		1 ± 2	10 ± 2	65 ± 0	–

crystalline CARV was dissolved in the same time unit. All Neusilin®-based products exhibited fast and complete drug release, with greater than 80% of drug dissolved in 10 min, which correlates with their good SME properties. Fast and almost complete drug release was obtained from the Aeroperl® 2:1 product, with 96% in 10 min. Similarly as in acidic media, drug release was faster from 2:1 products with ≥ 80% of CARV released from all carriers (presented in Fig. 5), which was attributed to the smaller droplet size of microemulsion in products with a higher SMEDDS:carrier ratio. Florite® R-based products exhibited slower and also less extensive drug release (maximum 88%). Syloid®-based products exhibited the slowest drug release profile, with the

exception of the Syloid® 2:1 product, for which the drug release was fast but incomplete; a maximum of 82% was achieved in 10 min. As shown in Section 3.2.2, incomplete dissolution cannot be attributed to the presence of crystalline CARV in s-SMEDDS. One possible explanation for slower drug release may be the smaller diameter of the pores (Syloid® 244FP) or entrance to the pores (Florite® R), which could impede a fast emulsification procedure and release of CARV-SMEDDS from the pores. Another possible explanation for slower drug release from Florite® R and Syloid® 244FP products may be partial adsorption of surfactant on the carrier. Due to partitioning of the drug in a surfactant-rich area, a lower amount of drug is released, which was the proposed explanation for slower drug (resveratrol) release from Syloid® 244FP-based s-SMEDDS in comparison with the Neusilin®-based product in the study by Bolko Seljak et al. (2018). This phenomenon would also explain the larger droplet size observed in our non-Neusilin®-based s-SMEDDS and incomplete drug release (82%) from the Syloid® 2:1 product. Slightly lower drug release extent from Syloid® and Florite® R 2:1 products was also observed at a pH of 1.2; however, it was less pronounced due to better solubility of CARV in acidic media. The reasons for incomplete drug release will be investigated in our future work.

3.2.4. Investigation of lower drug content and presence of impurities upon stability testing

For initial preliminary stability testing, the sample of the Syloid® 244FP 2:1 SD product was stored under accelerated conditions of 40 °C and 75% RH (in a container sealed in aluminum foil). After 1 month, the sample was visually assessed and CARV content determined. The stickiness of the sample and formation of some aggregates was observed, and the sample had a tendency to stick to the glass surface of the container. The CARV content dropped significantly (–28%); however, no additional peaks were observed on the HPLC chromatograms. Due to the unacceptable sample appearance and consistency (sticky agglomerates), all samples for stability testing were further stored at 20 to 25 °C and < 60% RH (hereinafter referred as controlled room conditions). A decrease in CARV content (–7%) was also observed in the Syloid® 244FP 2:1 product after storage at controlled room conditions for 2 months, with no additional peaks seen on HPLC chromatograms. Moisture uptake was not observed. The rapid drop of CARV content in s-SMEDDS was initially attributed to partial irreversible adsorption of SMEDDS to the porous silica-based carriers. However, the drop of CARV content in liquid SMEDDS (–3% after 1 month of storage at controlled room conditions),

which could not be explained with the formation of known CARV-related compounds, indicated the presence of unknown related substances. Examination of the chemical composition of SMEDDS raised suspicion that molecularly dispersed CARV molecules could react with the fatty acids present in the oily components of the SMEDDS formulation. Namely, CARV has a secondary amine functional group, which could form amides with carboxyl functional group of fatty acids. Due to their higher lipophilicity, these chemical compounds would have a large affinity to the reversed-phase chromatographic column used in HPLC determination of CARV content. Thus, slower elution of these amide compounds is expected, which could explain the absence of additional peaks on the chromatograms of CARV content analysis. The samples of Syloid® 244FP 1:1 and 2:1 that were stored under controlled room conditions for 3 months (Sy1-3mth and Sy2-3mth, respectively) and the sample of Syloid®244FP 2:1 stored under controlled room conditions for 7 months (Sy2-7mth) were submitted to LC-MS analysis to semi-quantitatively evaluate the potential content of amide impurities.

3.2.4.1. Development of the LC-MS Method. The chromatographic conditions of the LC-MS method were adopted from the HPLC method and adjusted as described in Section 2.14. Using the described gradient of the LC-MS method with improved eluting power, an additional peak at 51.9 min was detected. Its molecular weight $((M + H)^+ = 533.298)$ and elemental composition $(C_{32}H_{41}N_2O_5^+)$ were determined, after which the peak was analyzed using tandem MS. Its MS/MS spectrum (Fig. S2) featured several fragment ions that are characteristic of CARV and additional fragment ions, which suggests the presence of an unmodified hydroxyl group and a localized modification of the allylic part of the molecule. These data confirmed the presence of a newly discovered related substance of CARV (IMP1), which was structurally elucidated as an amide formed by CARV and octanoic acid (the reactional scheme can be seen in Fig. S3). Octanoic acid could be present in SMEDDS as an impurity or hydrolytic product (deesterified medium-chain fatty acids) in Capmul® MCM EP (mainly composed of mono- and diglycerides of C8 and C10 fatty acids).

The peak area of this related substance corresponded to approximately 5% of total content, which partially explains the lack of CARV determined in CARV content analysis. The LC-MS method was further modified (see Section 2.14) to achieve elution of other potential impurities/related substances formed by the reaction of CARV and fatty acids. Two additional chromatographic peaks were observed after elution of IMP1, with a retention time (RT) of 29.7 min (Fig. 6). After determination of their molecular mass and element composition, they were attributed to the amides of decanoic (IMP2, RT 32.2 min) and ricinoleic acid (IMP3, RT 33.2 min), which are present in the components of SMEDDS: Capmul® MCM EP and castor oil, respectively. The structural

formulas of the related substances detected are presented in Fig. 7.

The results indicate an increase in impurity formation with time because 4.3% of amides were determined in sample Sy2-4mth after 4 months of storage and 9.1% in sample Sy2-7mth, a batch of the same formulation prepared earlier, after 7 months of storage. This is expected because the amount of free fatty acids probably increases with time due to hydrolysis of acyl glycerides in SMEDDS. In addition, the nucleophilic secondary amine group of CARV could react with the carbonyl group of acyl glyceride, forming amide (Fig. S4).

Examples of CARV being incorporated into SMEDDS formulations for enhancement of drug release and bioavailability can be found in the literature (Mahmoud et al., 2009; Singh et al., 2013b); however, we have not found any data on CARV instability in SMEDDS formulations despite the presence of glycerides in the formulation. A possible explanation is that stability studies were insufficiently or inadequately conducted. The results of drug content and drug release, obtained by spectrophotometric analysis, could especially be unreliable because CARV and related substances absorb light at the same wavelengths. The HPLC method can separate peaks; however, it has to be developed to detect all related substances.

3.2.4.2. Stability Testing of S-SMEDDS. For further evaluation of CARV content and the increase in amide formation, conditions of the HPLC method were modified in accordance with chromatographic conditions of the LC-MS method. The HPLC sample chromatogram is presented in Fig. S5.

In chromatograms of freshly prepared SD product of Syloid® 244FP with a ratio of 2:1, no additional peaks were observed, only a peak belonging to CARV, indicating that the formation of amides does not occur due to the solidification or SMEDDS preparation process. The CARV content and share of amides and related substances in SD products with Syloid® 244FP at ratios of 1:1 and 2:1 was determined after 4 months, 6 months, and 8 Mmonths of storage at controlled room conditions. The percentage of CARV content was calculated taking into account initially determined CARV content (at 0 months storage time). To compare different solidification technologies, the Syloid® 244FP 2:1 product, produced via the adsorption method (ADS), was also analyzed after 4 months and 6 months of storage. The results of CARV content and share of known related substances and amide impurities are graphically presented in Fig. 8. The decrease in CARV content in all s-SMEDDS tested is graphically presented in Fig. S6.

After 4 months of storage, the largest decrease in CARV content was observed in the SD product of SMEDDS:Syloid® = 2:1. The presence of amides in a 4% share was determined; however, it could not explain the decrease in CARV content by almost 10%. The share of amide impurities in all products analyzed was 3 to 4%.

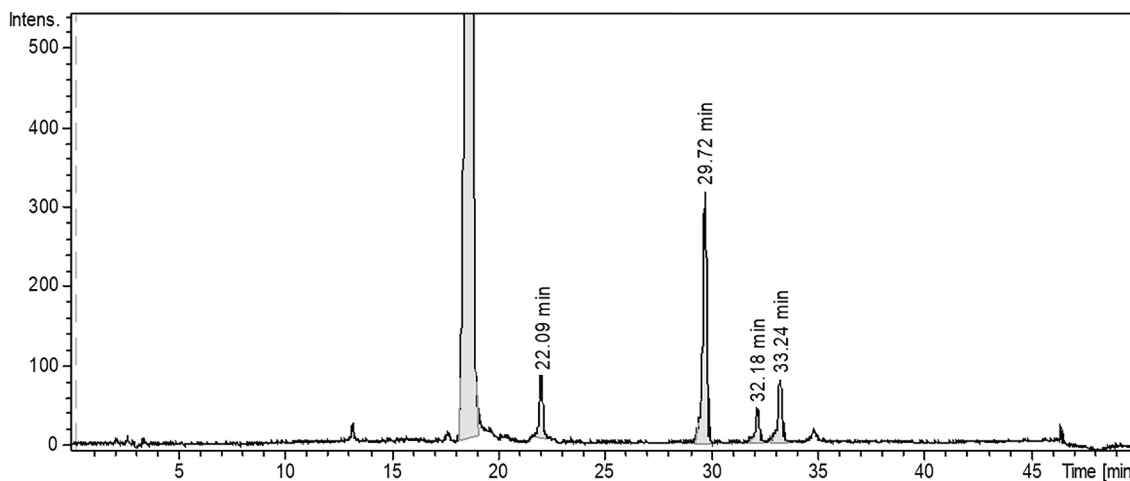


Fig. 6. Chromatogram of sample Sy2-7mth obtained by modified LC-MS chromatographic method.

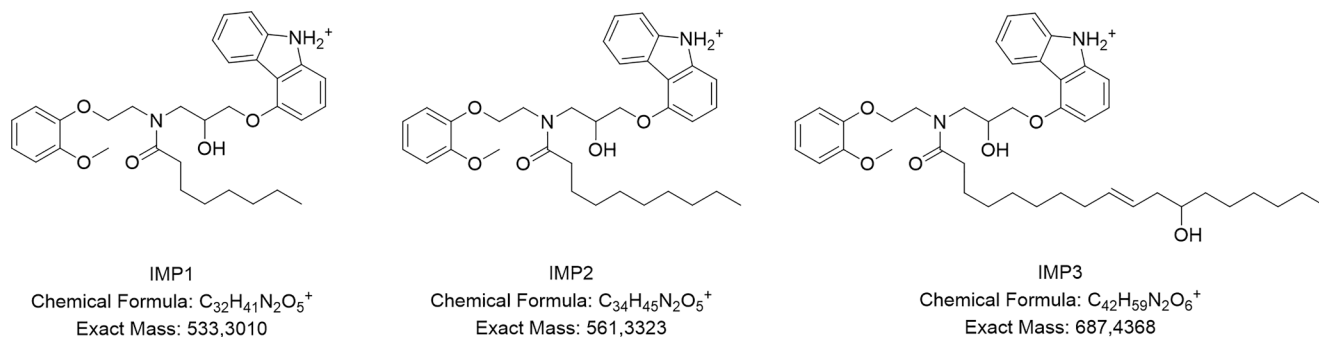


Fig. 7. Structural and chemical formulas of detected impurities and their molar mass (g/mol).

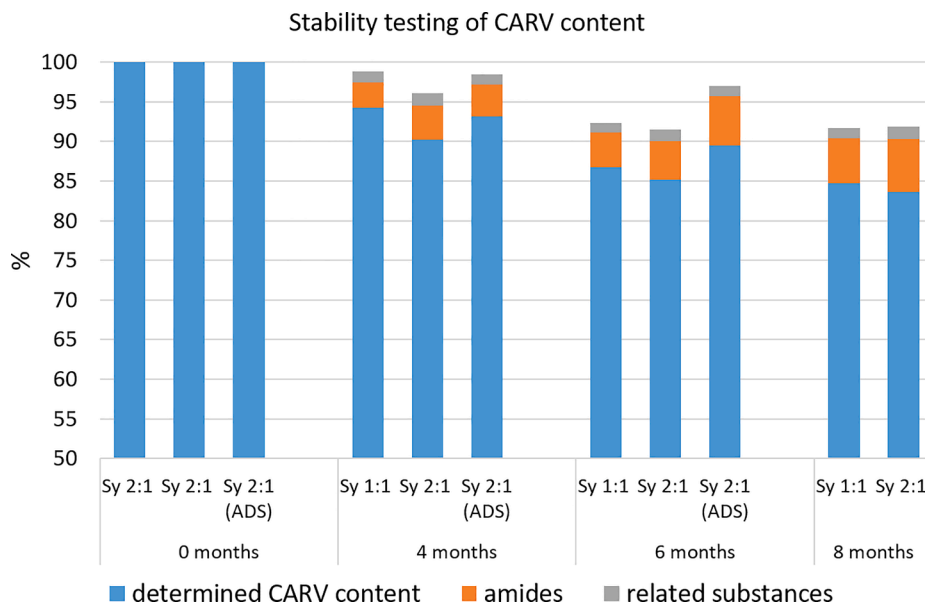


Fig. 8. Relative CARV content, share of amides and known related substances after 0, 4, 6 and 8 months of storage at controlled room conditions in s-SMEDDS obtained with SD (Syloid® 244FP 1:1 and 2:1) and s-SMEDDS Syloid® 244FP 1:1 obtained by adsorption method (ADS).

After 6 months of storage, the share of amides slightly increased (4–5%), whereas the CARV content decreased significantly more. Because the presence of impurities did not explain the total drop of CARV content in SD products (\cong 8% lack of CARV) and also in ADS products (3% lack of CARV), partial irreversible adsorption of SMEDDS in the pores of the carriers was introduced as another possible reason for the lower CARV content. To investigate this theory, another product was added to the stability testing after 6 months and 8 months of storage: an SD product of SMEDDS : (HPMC + Syloid® 244FP) = 1.5:1, produced with the carrier Syloid® 244FP, which had previously filled pores with HPMC. This product also exhibited a significant decrease in CARV content (88%) after 6 months of storage and, despite a smaller share of amides (2%), the lack of CARV was comparable to other SD products (–7%). Pore filling of Syloid® 244FP with drug-free SMEDDS in a ratio of 0.5:1 was also tested as means of enhancing relative CARV content. After 7 months of storage, this product exhibited the greatest decrease in CARV content (79%) and a slightly higher share of amide impurities (6%), which can be explained with a larger share of fatty acids available to react with CARV. In addition, the largest lack of CARV (12%) was observed, which indicates that either filling of deep regions of the pores with HPMC and especially with SMEDDS was unsuccessful or that another phenomenon, which was not observed in liquid CARV-SMEDDS, is responsible for the decrease in CARV content in s-SMEDDS.

After 8 months, the share of amides was 6 to 7% in all s-SMEDDS, and a slower CARV content decrease was observed (Fig. S6). Liquid

SMEDDS, on the other hand, exhibited a pronounced share of amides (15%). In addition, the SD product of Neusilin® US 2:1 after 8 months of storage was analyzed to investigate whether the CARV content is affected by the carrier type. The CARV content in this product was slightly higher (88% of initial CARV content) than in the Syloid® 244FP 2:1 product (84%), whereas the share of amides was comparable (8% vs. 7%). Nonetheless, a lack of CARV was observed (3%), but to a smaller extent than in the Syloid® 244FP 2:1 product (8%). The results indicate that choice of the carrier and solidification technology have an impact on CARV content during stability testing, with higher CARV content observed in the ADS product; however, no major differences in the formation of amide impurities were observed. A possible explanation for the observed decrease in CARV content, which cannot be explained solely with the formation of amide impurities, could be partial irreversible adsorption of the SMEDDS formulation or its components within the deep regions of the pores. In addition, the CARV and amide content in the Syloid® 244FP 2:1 product, obtained with SD dispersion stirred for 24 h prior to the SD process, was compared with the same formulation, where dispersion had been stirred for only 2 h prior to SD process. Product with longer mixing time of SD dispersion had a 3% lower content (85% vs. 82%) and a comparable share of amides (8%) after 8 months of storage. This could be explained with the theory that a longer time of contact between the SMEDDS dispersion and solid carrier results in lower CARV content due to penetration of SMEDDS deeper into the pores of the porous carrier. On the other hand, it is also possible that

other related substances are formed (e.g., diacylated CARV product with fatty acids reacting not only with the amine group but also with the hydroxyl group of CARV), which were not extracted from the chromatographic column with the mobile phase that was used. This remains to be investigated in a further study.

4. Conclusion

SD technology has been successfully used for the production of s-SMEDDS with high SMEDDS loading (up to 67% w/w), as products with SMEDDS:carrier ratio of 2:1 were produced.

In the initial experiments, the feed flow rate, drying gas flow rate, and atomization gas flow rate were adjusted to obtain a high-process yield. When the atomization gas flow rate was increased from 0.473 m³/h to 0.601 m³/h, the greatest improvement was achieved in the process yield (10–20%). The process yield was also influenced by the choice of carrier and the mixing time of the dispersion before SD. Because the porous carriers Syloid® 244FP, Neusilin® US2, Aeroperl® 300, and Florite® R were used, the process yield was improved with an increase in the mixing time of the SD dispersion. This was attributed to the more extensive adsorption of SMEDDS in the pores, when the contact time between the dispersion of SMEDDS and porous carrier was longer. Therefore, the particles with less SMEDDS on the surface had a lower tendency to stick to the walls of the drying chamber.

S-SMEDDS characteristics—drug loading, self-microemulsifying properties, and drug release rate and extent—were also affected by the choice of the carrier. Although all carriers reportedly exhibit a large and similar liquid adsorption capacity, differences in drug loading after SD were observed, which can be attributed to different pore size and length. None of the carriers can be identified as best because they had different impacts on the process yield, CARV content, and s-SMEDDS characteristics (self-emulsifying properties and drug release). All the SD products exhibited fast drug release due to the preserved SME properties and the absence of crystalline CARV.

Furthermore, the decrease in the content of CARV during storage time was investigated with the LC-MS method and was attributed to the formation of amides with fatty acids from the oily components of SMEDDS. The decreased carvedilol content that could not be explained solely with impurity formation was observed in s-SMEDDS produced with both solidification techniques: SD and ADS. A possible explanation could be partial irreversible adsorption of the SMEDDS formulation or its components within the deep regions of the pores, yet relative CARV content could not be increased with prefilling the pores of the carrier with drug-free SMEDDS or HPMC via the SD method. Further investigation of partial irreversible adsorption of SMEDDS in the porous carriers of SD products is necessary.

Finally, it is important to emphasize the finding that drugs with an amine functional group, such as our model drug CARV, are not suitable for incorporation into SMEDDS due to the formation of amides with fatty acids from the oily components of SMEDDS during storage time at room conditions. Moreover, when incorporating drugs with any nucleophilic functional group (such as alcohols), the formulation of SMEDDS should be carefully considered due to possible reactivity with free fatty acids or acyl glycerides.

CRedit authorship contribution statement

J. Mandić: Conceptualization, Methodology, Investigation, Visualization, Writing - original draft. **I. Kosmac:** Investigation. **M. Kovacević:** Investigation. **B. Hodnik:** Methodology, Investigation, Writing - original draft. **Ž. Hodnik:** Methodology, Investigation, Writing - original draft. **F. Vrečer:** Writing - review & editing, Resources, Supervision. **M. Gasperlin:** Funding acquisition, Writing - review & editing. **B. Perissutti:** Conceptualization, Writing - review & editing. **A. Zvonar Pobirk:** Conceptualization, Visualization, Writing - review & editing, Supervision, Project administration.

Declaration of Competing Interest

The authors declare that they have no known competing financial interests or personal relationships that could have appeared to influence the work reported in this paper.

Acknowledgement

This study was supported by Krka, d.d., Novo mesto, Slovenia and the Slovenian Research Agency, Slovenia (research core funding, no. P1-0189). M. De Piccoli is thanked for her help with the experimental work.

References

- Adler, C., 2017. *New Lipid-Based Formulation Approaches and Characterization Tools for Hot-Melt Extrusion* (dissertation). University of Basel.
- AEROPERL® 300 Pharma, Technical information 1414. <https://www.aerosil.com/product/aerosil/downloads/ti-1414-aeroperl-300-pharma-en.pdf> (accessed 24 April 2020).
- Aerosil, Evonik. <https://www.aerosil.com/product/aerosil/en/industries/pharmaceuticals/AEROPERL-300-Pharma> (accessed 24 April 2020).
- AEROSIL® and AEROPERL® Colloidal Silicon Dioxide for Pharmaceuticals Technical Information TI 1281. <https://www.aerosil.com/sites/lists/RE/Documents/SI/TI-1281-AEROSIL-and-AEROPERL-Colloidal-Silicon-Dioxide-for-Pharmaceuticals-EN.pdf> (accessed 24 April 2020).
- Agarwal, V., Siddiqui, A., Ali, H., Nazzal, S., 2009. Dissolution and powder flow characterization of solid self-emulsified drug delivery system (SEDDS). *Int. J. Pharm.* 366 (1-2), 44–52.
- Back, I.H., Ha, E.S., Yoo, J.W., Jung, Y., Kim, M.S., 2015. Design of a gelatin microparticle-containing self-microemulsifying formulation for enhanced oral bioavailability of dutasteride. *Drug. Des. Devel. Ther.* 9, 3231–3238.
- Bhandari, S., Rana, V., Tiwary, A.K., 2017. Antimalarial solid self-emulsifying system for oral use: in vitro investigation. *Ther. Deliv.* 8 (4), 201–213.
- Bolko Seljak, K., Ilić, I.G., Gašperlin, M., Zvonar Pobirk, A., 2018. Self-microemulsifying tablets prepared by direct compression for improved resveratrol delivery. *Int. J. Pharm.* 548 (1), 263–275.
- Brook, C.S., Chen, W., Spoons, P.G., 2007. Carvedilol phosphate salts and/or solvates thereof, corresponding compositions and/or methods of treatment. U.S. Patent 7,268,156.
- Čerpnjak, K., Zvonar, A., Gašperlin, M., Vrečer, F., 2013. Lipid-based systems as a promising approach for enhancing the bioavailability of poorly water-soluble drugs. *Acta Pharm.* 63 (4), 427–445.
- Čerpnjak, K., Zvonar, A., Vrečer, F., Gašperlin, M., 2015a. Characterization of naproxen-loaded solid SMEDDS prepared by spray drying: the effect of the polysaccharide carrier and naproxen concentration. *Int. J. Pharm.* 485 (1-2), 215–228.
- Čerpnjak, K., Pobirk, A.Z., Vrečer, F., Gašperlin, M., 2015b. Tablets and minitables prepared from spray-dried SMEDDS containing naproxen. *Int. J. Pharm.* 495 (1), 336–346.
- Chavan, R.B., Modi, S.R., Bansal, A.K., 2015. Role of solid carriers in pharmaceutical performance of solid supersaturable SEDDS of celecoxib. *Int. J. Pharm.* 495 (1), 374–384.
- Choudhari, Y., Reddy, U., Monsuur, F., Pauly, T., Hoefler, H., McCarthy, W., 2014. Comparative evaluation of porous silica based carriers for lipids and liquid drug formulations. *Mesoporous Biomater.* 1, 61–74.
- Florite, n.d. Tomita Pharmaceutical Co., Ltd. <http://www.tomitaph.co.jp/english/data/FLORITE.pdf> (accessed 24 April 2020).
- Fuji Chemical Industry Co., Ltd., 2007. Technical Newsletter. http://www.fujichemical.co.jp/english/newsletter/newsletter_pharma_0711.html (accessed 24 April 2020).
- Gonçalves, A., Nikmaram, N., Roohinejad, S., Estevinho, B.N., Rocha, F., Greiner, R., McClements, D.J., 2018. Production, properties, and applications of solid self-emulsifying delivery systems (S-SEDS) in the food and pharmaceutical industries. *Colloids Surf. A Physicochem. Eng. Asp.* 538, 108–126.
- Gumaste, S.G., Pawlak, S.A., Dalrymple, D.M., Nider, C.J., Trombetta, L.D., Serajuddin, A.T.M., 2013. Development of solid SEDDS, IV: effect of adsorbed lipid and surfactant on tableting properties and surface structures of different silicates. *Pharm. Res.* 30 (12), 3170–3185.
- Gumaste, S.G., Freire, B.O.S., Serajuddin, A.T.M., 2017a. Development of solid SEDDS, VI: effect of precoating of Neusilin® US2 with PVP on drug release from adsorbed self-emulsifying lipid-based formulations. *Eur. J. Pharm. Sci.* 110, 124–133.
- Gumaste, S.G., Serajuddin, A.T.M., 2017. Development of solid SEDDS, VII: effect of pore size of silica on drug release from adsorbed self-emulsifying lipid-based formulations. *Eur. J. Pharm. Sci.* 110, 134–147.
- Inugala, S., Eedara, B.B., Sunkavalli, S., Dhurke, R., Kandadi, P., Jukanti, R., Bandari, S., 2015. Solid self-nanoemulsifying drug delivery system (S-SNEDDS) of darunavir for

- improved dissolution and oral bioavailability: in vitro and in vivo evaluation. *Eur. J. Pharm. Sci.* 74, 1–10.
- Kang, J.H., Oh, D.H., Oh, Y.-K., Yong, C.S., Choi, H.-G., 2012. Effects of solid carriers on the crystalline properties, dissolution and bioavailability of flurbiprofen in solid self-nanoemulsifying drug delivery system (solid SNEDDS). *Eur. J. Pharm. Biopharm.* 80 (2), 289–297.
- Kim, M.S., Ha, E.S., Choo, G.H., Baek, I.H., 2015. Preparation and in vivo evaluation of a dutasteride-loaded solid-supersaturatable self-microemulsifying drug delivery system. *Int. J. Mol. Sci.* 16 (5), 10821–10833.
- Krupa, A., Szłęk, J., Jany, B.R., Jachowicz, R., 2015. Preformulation studies on solid self-emulsifying systems in powder form containing magnesium aluminometasilicate as porous carrier. *AAPS PharmSciTech.* 16 (3), 623–635.
- Li, L., Yi, T., Lam, C.W., 2013. Effects of spray-drying and choice of solid carriers on concentrations of Labrasol® and Transcutol® in solid self-microemulsifying drug delivery systems (SMEDDS). *Molecules.* 18 (1), 545–560.
- Mahmoud, E.A., Bendas, E.R., Mohamed, M.I., 2009. Preparation and evaluation of self-nanoemulsifying tablets of carvedilol. *AAPS Pharm. Sci. Tech.* 10 (1), 183–192.
- Mandić, J., Luštrik, M., Vrečer, F., Gasperlin, M., Zvonar Pobirk, A., 2019. Solidification of carvedilol loaded SMEDDS by swirling fluidized bed pellet coating. *Int. J. Pharm.* 566, 89–100.
- Mandić, J., Pirnat, V., Luštrik, M., German Ilić, I., Vrečer, F., Gasperlin, M., Zvonar Pobirk, A., 2020. Solidification of SMEDDS by fluid bed granulation and manufacturing of fast drug release tablets. *Int. J. Pharm.* 583, 119377. <https://doi.org/10.1016/j.ijpharm.2020.119377>.
- Mandić, J., Zvonar Pobirk, A., Vrečer, F., Gasperlin, M., 2017. Overview of solidification techniques for self-emulsifying drug delivery systems from industrial perspective. *Int. J. Pharm.* 533 (2), 335–345.
- Milović, M., Djuriš, J., Djekić, L., Vasiljević, D., Ibrić, S., 2012. Characterization and evaluation of solid self-microemulsifying drug delivery systems with porous carriers as systems for improved carbamazepine release. *Int. J. Pharm.* 436 (1-2), 58–65.
- Mura, P., Valleri, M., Mennini, N., 2012. New solid self-microemulsifying systems to enhance dissolution rate of poorly water soluble drugs. *Pharm. Dev. Technol.* 17 (3), 277–284.
- Oh, D.H., Kang, J.H., Kim, D.W., Lee, B.-J., Kim, J.O., Yong, C.S., Choi, H.-G., 2011. Comparison of solid self-microemulsifying drug delivery system (solid SMEDDS) prepared with hydrophilic and hydrophobic solid carrier. *Int. J. Pharm.* 420 (2), 412–418.
- Shazly, G., Mohsin, K., 2015. Dissolution improvement of solid self-emulsifying drug delivery systems of fenofibrate using an inorganic high surface adsorption material. *Acta Pharm.* 65 (1), 29–42.
- Singh, S.K., Vuddanda, P.R., Singh, S., Srivastava, A.K., 2013a. A comparison between use of spray and freeze drying techniques for preparation of solid self-microemulsifying formulation of valsartan and in vitro and in vivo evaluation. *Biomed. Res. Int.* 2013, 1–13.
- Singh, B., Singh, R., Bandyopadhyay, S., Kapil, R., Garg, B., 2013b. Optimized nanoemulsifying systems with enhanced bioavailability of carvedilol. *Colloids. Surf. B. Biointerfaces.* 101, 465–474.
- Snela, A., Jadach, B., Froelich, A., Skotnicki, M., Milczewska, K., Rojewska, M., Voelkel, A., Prochaska, K., Lulek, J., 2019. Self-emulsifying drug delivery systems with atorvastatin adsorbed on solid carriers: formulation and in vitro drug release studies. *Colloid Surface A.* 577, 281–290.
- Tan, A., Rao, S., Prestidge, C.A., 2013. Transforming lipid-based oral drug delivery systems into solid dosage forms: an overview of solid carriers, physicochemical properties, and biopharmaceutical performance. *Pharm. Res.* 30 (12), 2993–3017.
- Van Speybroeck, M., Williams, H.D., Nguyen, T.-H., Anby, M.U., Porter, C.J.H., Augustijns, P., 2012. Incomplete desorption of liquid excipients reduces the in vitro and in vivo performance of self-emulsifying drug delivery systems solidified by adsorption onto an inorganic mesoporous carrier. *Mol. Pharm.* 9 (9), 2750–2760.
- W. R. Grace & Co.-Conn., Technical Note 09/15. https://grace.com/pharma-and-biotech/en-us/Documents/Syloid/M309c_Syloid_FP_XDP_Tech_Note_0915.pdf (accessed 24 April 2020).
- Wang, J., Trinkle, D., Derbin, G., Martin, K., Sharif, S., Timmins, P., Desai, D., 2014. Moisture adsorption and desorption properties of colloidal silicon dioxide and its impact on layer adhesion of a bilayer tablet formulation. *J. Excip. Food Chem.* 5 (1), 21–31.
- Weerapol, Y., Limmatvapirat, S., Jansakul, C., Takeuchi, H., Sriamornsak, P., 2015. Enhanced dissolution and oral bioavailability of nifedipine by spontaneous emulsifying powders: effect of solid carriers and dietary state. *Eur. J. Pharm. Biopharm.* 91, 25–34.
- Yeom, D.W., Son, H.Y., Kim, J.H., Kim, S.R., Lee, S.G., Song, S.H., Chae, B.R., Choi, Y.W., 2016. Development of a solidified self-microemulsifying drug delivery system (S-SMEDDS) for atorvastatin calcium with improved dissolution and bioavailability. *Int. J. Pharm.* 506 (1-2), 302–311.